基于多重免疫组化技术探讨股骨头坏死愈胶囊治疗激素性股骨头坏死的作用机制

简羿[1],马茂潇[2],郭珈宜[2],刘又文[2],岳辰[2]

（1. 湖南中医药大学研究生院,湖南　长沙　410208;
2. 河南省洛阳正骨医院/河南省骨科医院,河南　洛阳　471002）

摘　要　目的:观察股骨头坏死愈胶囊治疗激素性股骨头坏死（steroid-induced osteonecrosis of femoral head,SONFH）的效果,基于多重免疫组化（multiplex immunohistochemistry,mIHC）技术探讨其治疗 SONFH 的作用机制。**方法:**将 100 只 SD 大鼠随机分为正常对照组、模型组、低剂量药物治疗组、高剂量药物治疗组。将模型组、低剂量药物治疗组、高剂量药物治疗组大鼠采用改良的脂多糖联合甲泼尼龙法建立 SONFH 模型。造模结束后,低剂量药物治疗组按照 0.33 g·kg^{-1}的剂量给予股骨头坏死愈胶囊溶液（将股骨头坏死愈胶囊粉剂溶于水中）灌胃,高剂量药物治疗组按照 0.67 g·kg^{-1}的剂量给予股骨头坏死愈胶囊溶液灌胃,正常对照组和模型组给予等量生理盐水灌胃。每日灌胃 2 次,连续治疗 4 周。治疗结束后,采用 Micro-CT 扫描分析大鼠股骨头松质骨微结构,组织切片染色观察大鼠股骨头组织病理学改变,并采用 mIHC 分析巨噬细胞极化及 Toll 样受体 4（Toll-like receptor 4,TLR4）/髓样分化因子初次应答基因 88（myeloid differentiation primary response gene 88,MyD88）/核因子-κB（nuclear factor-κB,NF-κB）信号通路相关蛋白表达。**结果:**①一般结果。模型组 1 只大鼠于造模后死亡,低剂量药物治疗组和高剂量药物治疗组分别有 3 只和 2 只大鼠在治疗过程中死亡。正常对照组大鼠精神状态良好、进食正常、毛发光泽无脱落,模型组、低剂量药物治疗组、高剂量药物治疗组大鼠在造模开始后第 3 天出现神情不振、进食减少、少量脱毛,1 周后精神、进食等逐渐恢复。②大鼠股骨头松质骨微结构 Micro-CT 扫描分析结果。模型组大鼠股骨头松质骨骨体积分数、骨小梁厚度、骨小梁数量小于正常对照组（$P=0.000$,$P=0.000$,$P=0.000$）,骨小梁分离度大于正常对照组（$P=0.000$）;低剂量药物治疗组大鼠股骨头松质骨骨体积分数、骨小梁厚度与模型组的差异均无统计学意义（$P=0.052$,$P=0.071$）,骨小梁数量大于模型组（$P=0.012$）,骨小梁离散度小于模型组（$P=0.001$）;高剂量药物治疗组大鼠股骨头松质骨骨体积分数、骨小梁厚度、骨小梁数量大于模型组（$P=0.001$,$P=0.011$,$P=0.000$）,骨小梁离散度小于模型组（$P=0.001$）,骨体积分数、骨小梁厚度、骨小梁数量、骨小梁离散度与低剂量药物治疗组的差异均无统计学意义（$P=0.146$,$P=0.414$,$P=0.086$,$P=0.146$）。③大鼠股骨头组织病理学观察结果。模型组大鼠股骨头空骨陷窝率、骨坏死发生率均高于正常对照组（$P=0.000$,$P=0.000$）;低剂量药物治疗组大鼠股骨头空骨陷窝率低于模型组（$P=0.000$）,骨坏死发生率与模型组的差异无统计学意义（$P=0.054$）;高剂量药物治疗组大鼠股骨头空骨陷窝率和骨坏死发生率均低于模型组（$P=0.000$,$P=0.000$）,空骨陷窝率低于低剂量药物治疗组（$P=0.049$）,骨坏死发生率与低剂量药物治疗组的差异无统计学意义（$P=0.556$）。④巨噬细胞极化 mIHC 分析结果。模型组大鼠股骨头 M1 型巨噬细胞、M2 型巨噬细胞占比均高于正常对照组（$P=0.000$,$P=0.000$）;低剂量药物治疗组大鼠股骨头 M1 型巨噬细胞、M2 型巨噬细胞占比与模型组的差异均无统计学意义（$P=0.270$,$P=0.533$）;高剂量药物治疗组大鼠股骨头 M1 型巨噬细胞占比低于模型组（$P=0.009$）,与低剂量药物治疗组的差异无统计学意义（$P=0.131$）,M2 型巨噬细胞占比高于模型组和低剂量药物治疗组（$P=0.006$,$P=0.038$）。⑤TLR4/MyD88/NF-κB 信号通路蛋白表达 mIHC 分析结果。模型组大鼠股骨头 TLR4、MyD88、NF-κB p65 蛋白相对表达量均高于正常对照组（$P=0.000$,$P=0.000$,$P=0.000$）;低剂量药物治疗组大鼠股骨头 TLR4、MyD88 蛋白相对表达量与模型组的差异均无统计学意义（$P=0.268$,$P=0.280$）,NF-κB p65 蛋白相对表达量低于模型组（$P=0.034$）;高剂量药物治疗组 TLR4、MyD88、NF-κB p65 蛋白相对表达量均低于模型组和低剂量药物治疗组（TLR4:$P=0.002$,$P=0.040$;MyD8:$P=0.000$,$P=0.013$;NF-κB p65:$P=0.000$,$P=0.039$）。**结论:**股骨头坏死愈胶囊治疗 SONFH,能够显著改善股骨头骨微结构、抑制骨坏死,其作用具有一定的剂量依赖性;其作用机制与调控 TLR4/MyD88/NF-κB 信号通路及巨噬细胞极化有关。

关键词　股骨头坏死;激素类;股骨头坏死愈胶囊;免疫组织化学;巨噬细胞;信号传导

基金项目:国家自然科学基金项目（82074472）;2022 年度河洛青年人才托举工程项目（2022HLTJ15）

通讯作者:岳辰　E-mail:Orthopedics. Yue@ outlook. com

The mechanism of Gugutou Huaisiyu Jiaonang(股骨头坏死愈胶囊) in treatment of steroid-induced osteonecrosis of femoral head: a multiplex immunohistochemistry technique-based experimental study

JIAN Yi[1], MA Maoxiao[2], GUO Jiayi[2], LIU Youwen[2], YUE Chen[2]

1. Postgraduate College of Hunan University of Chinese Medicine, Changsha 410208, Hunan, China

2. Luoyang Orthopedic-Traumatological Hospital, Luoyang 471002, Henan, China

ABSTRACT **Objective**: To observe the outcome of Gugutou Huaisiyu Jiaonang(股骨头坏死愈胶囊, GGTHSYJN) in treatment of steroid-induced osteonecrosis of femoral head(SONFH), and to explore its underlying mechanism via multiplex immunohistochemistry(mIHC) technique. **Methods**: One hundred Sprague-Dawley(SD) rats were randomly assigned into normal control group, model group, low-dose drug treatment group and high-dose drug treatment group. After adaptive feeding for one week, the rats in model group, low-dose drug treatment group and high-dose drug treatment group were subjected to intramuscular injection of lipopolysaccharide and methylprednisolone in turn for inducing SONFH. After the end of modeling, the rats in low-dose drug treatment group were intragastric administrated with 0.33 g/kg GGTHSYJN solution(GGTHSYJN powders were dissolved into water), the ones in high-dose drug treatment group with 0.67 g/kg GGTHSYJN solution, while the ones in normal control group and model group with the same dose of normal saline. All rats in the 4 groups were intragastric administrated twice a day for consecutive 4 weeks. After the end of treatment, the femur heads were harvested from the rats, and the cancellous bone microstructure of femur head was observed and analyzed by using Micro-CT scanning; meanwhile, the tissue sections of femur head were stained with hematoxylin-eosin(HE) for observing the histopathological changes. Furthermore, the macrophage polarization and the expressions of Toll-like receptor 4(TLR4)/myeloid differentiation primary response gene 88(MyD88)/nuclear factor-κB(NF-κB) signaling pathway-related protein were analyzed by using mIHC technique. **Results**: ①One rat in model group died after the modeling, and 3 rats in low-dose drug treatment group and 2 ones in high-dose drug treatment group died during the treatment. Rats with good mental state, normal eating and drinking as well as healthy fur without shedding were observed in normal group. On day 3 after the beginning of the modeling, the rats in model group, low-dose drug treatment group, and high-dose drug treatment group gradually exhibited the symptoms as dispiritedness, reduced eating and drinking, as well as slight hair removal, and the signs gradually recovered after one week. ②The normal control group exhibited higher bone volume fraction(BVF), thicker trabeculae, more trabeculae, and lower trabecular separation(Tb. Sp) in cancellous bone compared with that of model group($P=0.000$, $P=0.000$, $P=0.000$, $P=0.000$). The differences in BVF and trabecular thickness were not statistically significant between low-dose drug treatment group and model group($P=0.052$, $P=0.071$), while, the trabeculae was more and the Tb. Sp was lower in low-dose drug treatment group compared to model group($P=0.012$; $P=0.001$). The high-dose drug treatment group displayed higher BVF, thicker trabeculae, more trabeculae, and lower Tb. Sp in cancellous bone compared with that of model group($P=0.001$, $P=0.011$, $P=0.000$, $P=0.001$), while, in contrast to that of low-dose drug treatment group, the results revealed no significant differences($P=0.146$, $P=0.414$, $P=0.086$, $P=0.146$). ③The percentage of empty lacunae and the incidence rate of osteonecrosis in femur heads were higher in model group compared to normal control group($P=0.000$, $P=0.000$). The percentage of empty lacunae in femur head was lower in low-dose drug treatment group compared to model group($P=0.000$), while, the comparison of osteonecrosis incidence rate between the 2 groups revealed no significant difference($P=0.054$). The percentage of empty lacunae and the incidence rate of osteonecrosis in femur heads were lower in high-dose drug treatment group compared to model group($P=0.000$, $P=0.000$); furthermore, the percentage of empty lacunae was lower in high-dose drug treatment group compared to low-dose drug treatment group($P=0.049$), while, the comparison of osteonecrosis incidence rate between the 2 groups revealed no significant difference($P=0.556$). ④The M1 macrophages and M2 macrophages accounted for a higher proportion in femur heads of rats in model group compared to normal control group($P=0.000$, $P=0.000$). There was no statistical difference in the proportions of M1 macrophages and M2 macrophages between low-dose drug treatment group and model group($P=0.270$, $P=0.533$). The M1 macrophages accounted for a lower proportion in high-dose drug treatment group compared to model group($P=0.009$), while the M2 macrophages accounted for a higher proportion in high-dose drug treatment group compared to model group and low-dose drug treatment group($P=0.006$, $P=0.038$); furthermore, the comparison of the proportion of M1 macrophages between high-dose drug treatment group and low-dose drug treatment group revealed no significant difference($P=0.131$). ⑤The relative expression levels of TLR4, MyD88 and NF-κB p65 protein in femur heads were higher in model group compared to normal control group($P=0.000$, $P=0.000$, $P=0.000$). There was no statistical difference in the relative expression levels of TLR4 and MyD88 protein between low-dose drug treatment group and model group($P=0.268$, $P=0.280$), while the relative expression level of NF-κB p65 protein was lower in low-dose drug treatment group compared to model group($P=0.034$). The relative expression levels

of TLR4,MyD88 and NF-κB p65 protein were lower in high-dose drug treatment group compared to model group and low-dose drug treatment group(TLR4:$P=0.002$,$P=0.040$;MyD88:$P=0.000$,$P=0.013$;NF-κB p65:$P=0.000$,$P=0.039$). **Conclusion**:GGTHSYJN can significantly improve the bone microstructure of femur head and inhibit osteonecrosis in treatment of SONFH,and it exhibits dose-dependence in the efficacy. It may work by regulating TLR4/MyD88/NF-κB signaling pathway and macrophage polarization.

Keywords　femur head necrosis;hormones;Gugutou Huaisiyu Jiaonang;immunohistochemistry;macrophages;signal transduction

股骨头坏死是骨科临床中常见的高致残性疾病之一,创伤、酗酒及激素滥用等是引起股骨头坏死的主要因素[1]。我国股骨头坏死患者中约有 1/4 为激素滥用引起[2]。对于早期激素性股骨头坏死(steroid-induced osteonecrosis of femoral head,SONFH)患者,如不能采取有效的干预措施,多数患者会在 5 年内发生股骨头塌陷、坏死[3]。股骨头坏死愈胶囊是平乐郭氏正骨治疗“骨蚀”的经典方剂,具有补益肝肾、活血化瘀的作用。我们团队前期研究发现,股骨头坏死愈胶囊具有改善髋关节功能、减缓 SONFH 发病进程、降低股骨颈骨折内固定术后股骨头坏死发生率的作用[4-5]。但股骨头坏死愈胶囊治疗 SONFH 的作用机制尚不清楚。多重免疫组化(multiplex immunohistochemistry,mIHC)是一项先进的病理学检测技术,在推演上下游信号通路、探索药物作用机制方面具有一定的优势[6]。目前,mIHC 已被广泛应用于肿瘤、心血管疾病、肠道疾病等的机制研究[7-9]。我们前期采用 mIHC 成功揭示了非创伤性股骨头坏死巨噬细胞异常极化的相关机制[10]。为了探讨股骨头坏死愈胶囊治疗 SONFH 的作用机制,我们建立了 SONFH 大鼠模型,并采用 mIHC 进行了相关实验研究,现总结报告如下。

1　材料与仪器

1.1　实验动物

无特定病原 SD 大鼠 100 只,购自成都达硕实验动物有限公司[生产许可 SCXK(川)2020-0030]。实验方案经河南省洛阳正骨医院(河南省骨科医院)伦理委员会审查通过,伦理批件号:KY2021-007-01。

1.2　实验药物

股骨头坏死愈胶囊[河南省洛阳正骨医院(河南省骨科医院)院内制剂,批号:20200209;规格:每粒装 0.35 g]。

1.3　实验试剂

甲泼尼龙、苏木素(北京索莱宝科技有限公司),脂多糖(美国 Sigma 公司),10% 中性福尔马林[康迪斯化工(湖北)有限公司],Opal 多色荧光免疫组化标记试剂盒(美国 Akoya Biosciences 公司),CD68、CD80、Toll 样受体 4(Toll-like receptor 4,TLR4)、髓样分化因子初次应答基因 88(myeloid differentiation primary response gene 88,MyD88)、核因子-κB(nuclear factor-κB,NF-κB)p65 抗体(美国 Abcam 公司),CD206 抗体(美国 Thermo 公司)。

1.4　实验仪器

HM 340E 石蜡切片机、TLZ11 摊片仪、ClearVue 全自动封片仪(美国 Thermo 公司),BX51 光学显微镜(日本 Olympus 公司),vivaCT40 Micro-CT(瑞士 SCANCO Medical AG 公司)。

2　方　法

2.1　分组方法

将 100 只大鼠称重后按体质量排序编号,从随机数字表中抄录 100 个连续的 2 位数记录在大鼠编号下方,将随机数字除以 4,余数为 1 的随机数字对应的大鼠纳入正常对照组,余数为 2 的随机数字对应的大鼠纳入模型组,余数为 3 的随机数字对应的大鼠纳入低剂量药物治疗组,整除的随机数字对应的大鼠纳入高剂量药物治疗组。若分配不均,则继续抄录随机数字并采用余数法进行调整。

2.2　大鼠 SONFH 造模方法

大鼠适应性饲养 1 周后,将模型组、低剂量药物治疗组、高剂量药物治疗组大鼠采用改良的脂多糖联合甲泼尼龙法建立 SONFH 模型[11]:按照 10 μg·kg^{-1}的剂量给 SD 大鼠肌肉注射脂多糖,共注射 2 次,2 次间隔 7 d,第 2 次注射脂多糖 24 h 后,按照 25 mg·kg^{-1}的剂量给 SD 大鼠肌肉注射甲泼尼龙,每日注射 1 次,连续注射 3 d。

2.3　治疗方法

造模结束后,低剂量药物治疗组按照 0.33 g·kg^{-1}的剂量给予股骨头坏死愈胶囊溶液(将股骨头坏死愈胶囊粉剂溶于水中)灌胃,高剂量药物治疗组按照 0.67 g·kg^{-1}的剂量给予股骨头坏死愈胶囊溶液灌

胃,正常对照组和模型组给予等量生理盐水灌胃。每日灌胃 2 次,连续治疗 4 周。药物等效剂量均按照人体与 SD 大鼠的体表面积进行换算。

2.4　评价方法

2.4.1　Micro-CT 扫描分析大鼠股骨头松质骨微结构　治疗结束后,腹腔注射 3% 的戊巴比妥钠麻醉大鼠,分离大鼠双侧股骨,注意避免股骨头软骨损伤。将大鼠股骨固定于 4% 多聚甲醛中 24 h 后,再置于 0.9% 生理盐水中浸泡 24 h。采用 vivaCT40 Micro-CT 对大鼠股骨进行扫描,并进行三维重建。采用仪器自带软件分析股骨头松质骨的骨微结构,并提取大鼠股骨头松质骨的骨体积分数、骨小梁厚度、骨小梁数量(1 mm 线段与骨小梁交点的个数)及骨小梁分离度(骨小梁之间的平均距离)等指标。

2.4.2　组织切片染色观察大鼠股骨头组织病理学改变　将大鼠股骨浸入 10% 中性福尔马林中浸泡固定 48 h,常规脱钙、脱水、石蜡包埋、切片。取股骨头组织切片,采用 HE 染色观察股骨头组织病理学改变,计算空骨陷窝率和骨坏死发生率:在 200 倍镜下随机选取 10 个视野,计算每个视野中骨小梁空骨陷窝数与骨小梁细胞数的比值,10 个视野比值的平均值即为空骨陷窝率;当空骨陷窝率 > 50%,提示发生股骨头坏死,任一侧发生股骨头坏死的大鼠数量与组内大鼠数量的比值即为骨坏死发生率。

2.4.3　mIHC 检测巨噬细胞极化及 TLR4/MyD88/NF-κB 信号通路相关蛋白表达　取股骨头组织石蜡切片,脱蜡水化后,加入 EDTA 抗原修复液,于微波高火下修复抗原;加入抗原封闭液,室温封闭 10 min;加入 CD206 一抗(抗体稀释比例为 1∶200),4 ℃孵育过夜;PBS 缓冲液漂洗后,加入 Opal Polymer HRP 抗鼠/兔通用型二抗,37 ℃孵育 10min;PBS 缓冲液避光漂洗后,加入 Opal520 试剂室温显色 10 min。再次加入 EDTA 抗原修复液,于微波高火下修复抗原,按照上述步骤依次完成 CD68(抗体稀释比例为 1∶200)、CD80(抗体稀释比例为 1∶100)、TLR4(抗体稀释比例为 1∶100)、MyD88(抗体稀释比例为 1∶100)、NF-κB P65(抗体稀释比例为 1∶200)的标记和显色。完成所有蛋白的标记和显色后,PBS 缓冲液避光漂洗,滴加 DAPI 染料,避光孵育 5 min;双蒸水避光漂洗后,加入防淬灭剂后,封片。于荧光显微镜下观察切片,采用 Qupath 0.3.4 软件统计 CD206、CD68、CD80、TLR4、MyD88、NF-κB P65 的荧光强度,分析 CD206、CD68、CD80、TLR4、MyD88、NF-κB P65 的蛋白相对表达量,并计算 M1 型巨噬细胞、M2 型巨噬细胞的占比。M1 型巨噬细胞占比 = CD80 的相对荧光强度/CD68 的相对荧光强度 ×100%,M2 型巨噬细胞占比 = CD206 的相对荧光强度/CD68 的相对荧光强度 ×100%。

2.5　数据统计

采用 SPSS25.0 统计软件对所得数据进行统计学分析。骨体积分数、骨小梁厚度、骨小梁数量、骨小梁分离度、空骨陷窝率、M1 型巨噬细胞占比、M2 型巨噬细胞占比及 TLR4、MyD88、NF-κB p65 蛋白相对表达量的组间比较均采用单因素方差分析,组间两两比较均采用 LSD-t 检验;骨坏死发生率的组间比较采用卡方检验,两两比较采用卡方分割法。检验水准 $\alpha = 0.05$,卡方分割检验水准 $\alpha' = 0.012\ 5$。

3　结　果

3.1　一般结果

模型组 1 只大鼠于造模后死亡,低剂量药物治疗组和高剂量药物治疗组分别有 3 只和 2 只大鼠在治疗过程中死亡。正常对照组大鼠精神状态良好、进食正常、毛发光泽无脱落,模型组、低剂量药物治疗组、高剂量药物治疗组大鼠在造模开始后第 3 天出现神情不振、进食减少、少量脱毛,1 周后精神、进食等逐渐恢复。

3.2　大鼠股骨头松质骨微结构 Micro-CT 扫描分析结果

大鼠股骨近端 CT 片显示,正常对照组股骨头松质骨的骨小梁呈多孔网架结构,排列规律,骨小梁数量、厚度正常;模型组骨小梁明显减少、变细,稀疏,排列不规律;高剂量药物治疗组骨小梁较模型组增厚、变粗,致密,排列规律;低剂量药物治疗组大鼠股骨头松质骨微结构表现介于模型组与高剂量药物治疗组之间(图 1)。正常对照组、模型组、低剂量药物治疗组、高剂量药物治疗组大鼠股骨头松质骨骨体积分数、骨小梁厚度、骨小梁数量、骨小梁分离度组间比较,差异均有统计学意义。模型组、低剂量药物治疗组、高剂量药物治疗组大鼠股骨头松质骨骨体积分数、骨小梁厚度、骨小梁数量均小于正常对照组(骨体积分数:$P = 0.000$,$P = 0.000$,$P = 0.000$;骨小梁厚

度：$P=0.000$，$P=0.003$，$P=0.026$；骨小梁数量：$P=0.000$，$P=0.000$，$P=0.031$），骨小梁分离度均大于正常对照组（$P=0.000$，$P=0.001$，$P=0.036$）；低剂量药物治疗组大鼠股骨头松质骨骨体积分数、骨小梁厚度与模型组的差异均无统计学意义（$P=0.052$，$P=0.071$），骨小梁数量大于模型组（$P=0.012$），骨小梁离散度小于模型组（$P=0.001$）；高剂量药物治疗组大鼠股骨头松质骨骨体积分数、骨小梁厚度、骨小梁数量大于模型组（$P=0.001$，$P=0.011$，$P=0.000$），骨小梁离散度小于模型组（$P=0.001$），骨体积分数、骨小梁厚度、骨小梁数量、骨小梁离散度与低剂量药物治疗组的差异均无统计学意义（$P=0.146$，$P=0.414$，$P=0.086$，$P=0.146$）。见表 1。

3.3　大鼠股骨头组织病理学观察结果

HE 染色结果显示，正常对照组大鼠股骨头骨小梁内无明显空骨陷窝，细胞核正常；模型组、低剂量药物治疗组及高剂量药物治疗组大鼠股骨头骨小梁内出现不同程度的空骨陷窝，细胞核变小、萎缩并移动到细胞边缘，且以模型组最为明显（图 2）。正常对照组、模型组、低剂量药物治疗组、高剂量药物治疗组大鼠股骨头空骨陷窝率、骨坏死发生率组间比较，差异均有统计学意义。模型组、低剂量药物治疗组、高剂量药物治疗组大鼠股骨头空骨陷窝率、骨坏死发生率均高于正常对照组（空骨陷窝率：$P=0.000$，$P=0.000$，$P=0.000$；骨坏死发生率：$P=0.000$，$P=0.000$，$P=0.000$）；低剂量药物治疗组大鼠股骨头空骨陷窝率低于模型组（$P=0.000$），骨坏死发生率与模型组的差异无统计学意义（$P=0.054$）；高剂量药物治疗组大鼠股骨头空骨陷窝率和骨坏死发生率均低于模型组（$P=0.000$，$P=0.000$），空骨陷窝率低于低剂量药物治疗组（$P=0.049$），骨坏死发生率与低剂量药物治疗组的差异无统计学意义（$P=0.556$）。见表 2。

3.4　巨噬细胞极化 mIHC 检测结果

正常对照组、模型组、低剂量药物治疗组、高剂量药物治疗组大鼠股骨头 M1 型巨噬细胞、M2 型巨噬细胞占比组间比较，差异均有统计学意义。模型组、低剂量药物治疗组、高剂量药物治疗组大鼠股骨头 M1 型巨噬细胞、M2 型巨噬细胞占比均高于正常对照组（M1 型巨噬细胞占比：$P=0.000$，$P=0.000$，$P=0.000$；M2 型巨噬细胞占比：$P=0.000$，$P=0.000$，$P=0.000$）；低剂量药物治疗组大鼠股骨头 M1 型巨噬细胞、M2 型巨噬细胞占比与模型组的差异均无统计学意义（$P=0.270$，$P=0.533$）；高剂量药物治疗组大鼠股骨头 M1 型巨噬细胞占比低于模型组（$P=0.009$），M2 型巨噬细胞占比高于模型组（$P=0.006$）；高剂量药物治疗组大鼠股骨头 M1 型巨噬细胞占比与低剂量药物治疗组的差异无统计学意义（$P=0.131$），M2 型巨噬细胞占比高于低剂量药物治疗组（$P=0.038$）。见表 3、图 3。

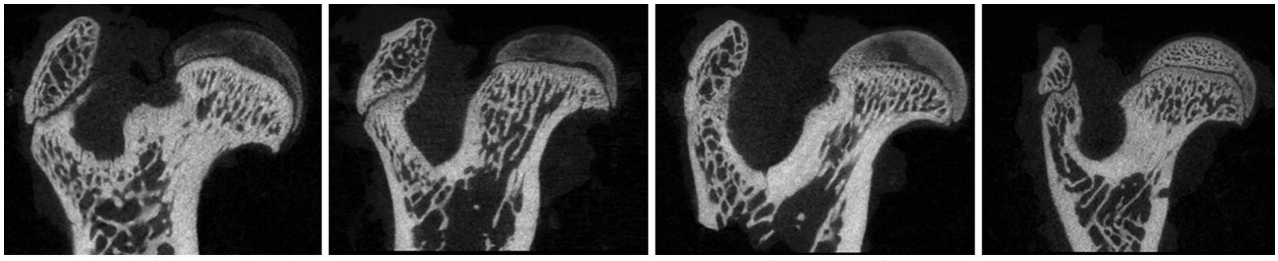

(1) 正常对照组　(2) 模型组　(3) 低剂量药物治疗组　(4) 高剂量药物治疗组

图 1　4 组大鼠股骨近端 CT 片

表 1　4 组大鼠股骨头松质骨微结构 Micro-CT 扫描分析结果

组别	样本量/只	骨体积分数/（$\bar{x}\pm s$，%）	骨小梁厚度/（$\bar{x}\pm s$，mm）	骨小梁数量/（$\bar{x}\pm s$，个·mm^{-1}）	骨小梁分离度/（$\bar{x}\pm s$，mm）
正常对照组	25	63.78±15.99	0.25±0.08	2.58±0.37	0.14±0.07
模型组	24	18.75±9.90	0.11±0.04	1.52±0.39	0.59±0.19
低剂量药物治疗组	22	33.33±11.19	0.16±0.04	1.94±0.30	0.36±0.11
高剂量药物治疗组	23	44.11±23.95	0.19±0.08	2.22±0.36	0.27±0.14
F 值		13.661	8.605	15.831	18.901
P 值		0.000	0.000	0.000	0.000

3.5　TLR4/MyD88/NF-κB 信号通路相关蛋白表达 mIHC 检测结果

正常对照组、模型组、低剂量药物治疗组、高剂量药物治疗组大鼠股骨头 TLR4、MyD88、NF-κB p65 的蛋白相对表达量组间比较,差异均有统计学意义。模型组、低剂量药物治疗组、高剂量药物治疗组大鼠股骨头 TLR4、MyD88、NF-κB p65 蛋白相对表达量均高于正常对照组(TLR4 蛋白相对表达量:$P=0.000$,$P=0.000$,$P=0.028$;MyD88 蛋白相对表达量:$P=0.000$,$P=0.000$,$P=0.001$;NF-κB p65 蛋白相对表达量:$P=0.000$,$P=0.000$,$P=0.001$);低剂量药物治疗组大鼠股骨头 TLR4、MyD88 蛋白相对表达量与模型组的差异均无统计学意义($P=0.268$,$P=0.280$),NF-κB p65 蛋白相对表达量低于模型组($P=0.034$);高剂量药物治疗组 TLR4、MyD88、NF-κB p65 蛋白相对表达量均低于模型组和低剂量药物治疗组(TLR4 蛋白相对表达量:$P=0.002$,$P=0.040$;MyD88 蛋白相对表达量:$P=0.000$,$P=0.013$;NF-κB p65 蛋白相对表达量:$P=0.000$,$P=0.039$)。见表 4、图 3。

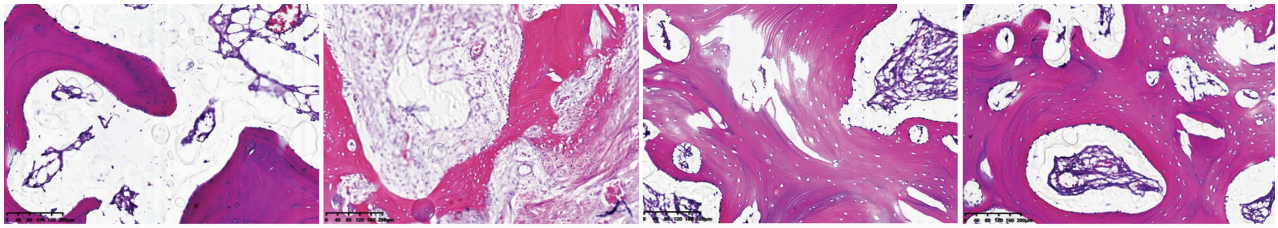

(1) 正常对照组　(2) 模型组　(3) 低剂量药物治疗组　(4) 高剂量药物治疗组

图 2　4 组大鼠股骨头组织切片 HE 染色结果(×200)

表 2　4 组大鼠股骨头空骨陷窝率和骨坏死发生率

组别	样本量/只	空骨陷窝率/($\bar{x}\pm s$,%)	骨坏死发生率/%
正常对照组	25	12.27±4.12	0
模型组	24	61.97±13.14	83.3
低剂量药物治疗组	22	50.92±14.17	54.5
高剂量药物治疗组	23	46.91±13.33	43.5
检验统计量		$F=244.316$	$\chi^2=35.579$
P 值		0.000	0.000

表 3　4 组大鼠股骨头巨噬细胞极化检测结果

组别	样本量/只	M1 型巨噬细胞占比/($\bar{x}\pm s$,%)	M2 型巨噬细胞占比/($\bar{x}\pm s$,%)
正常对照组	25	6.95±3.64	7.60±3.14
模型组	24	28.18±15.34	17.82±6.95
低剂量药物治疗组	22	24.86±10.51	19.02±6.94
高剂量药物治疗组	23	20.25±7.46	23.13±8.21
F 值		24.749	4.602
P 值		0.000	0.000

表 4　4 组大鼠股骨头 TLR4/MyD88/NF-κB 信号通路相关蛋白相对表达量

组别	样本量/只	TLR4[1)]($\bar{x}\pm s$)	MyD88[2)]($\bar{x}\pm s$)	NF-κB p65[3)]($\bar{x}\pm s$)
正常对照组	25	1.06±0.27	1.06±0.33	1.11±0.42
模型组	24	1.85±0.54	2.53±0.76	2.77±0.83
低剂量药物治疗组	22	1.69±0.62	2.31±0.85	2.29±0.89
高剂量药物治疗组	23	1.38±0.51	1.78±0.73	1.83±0.76
F 值		12.062	22.203	21.623
P 值		0.000	0.000	0.000

注:1)Toll 样受体-4;2)髓样分化因子初次应答基因 88;3)核因子-κB p65。

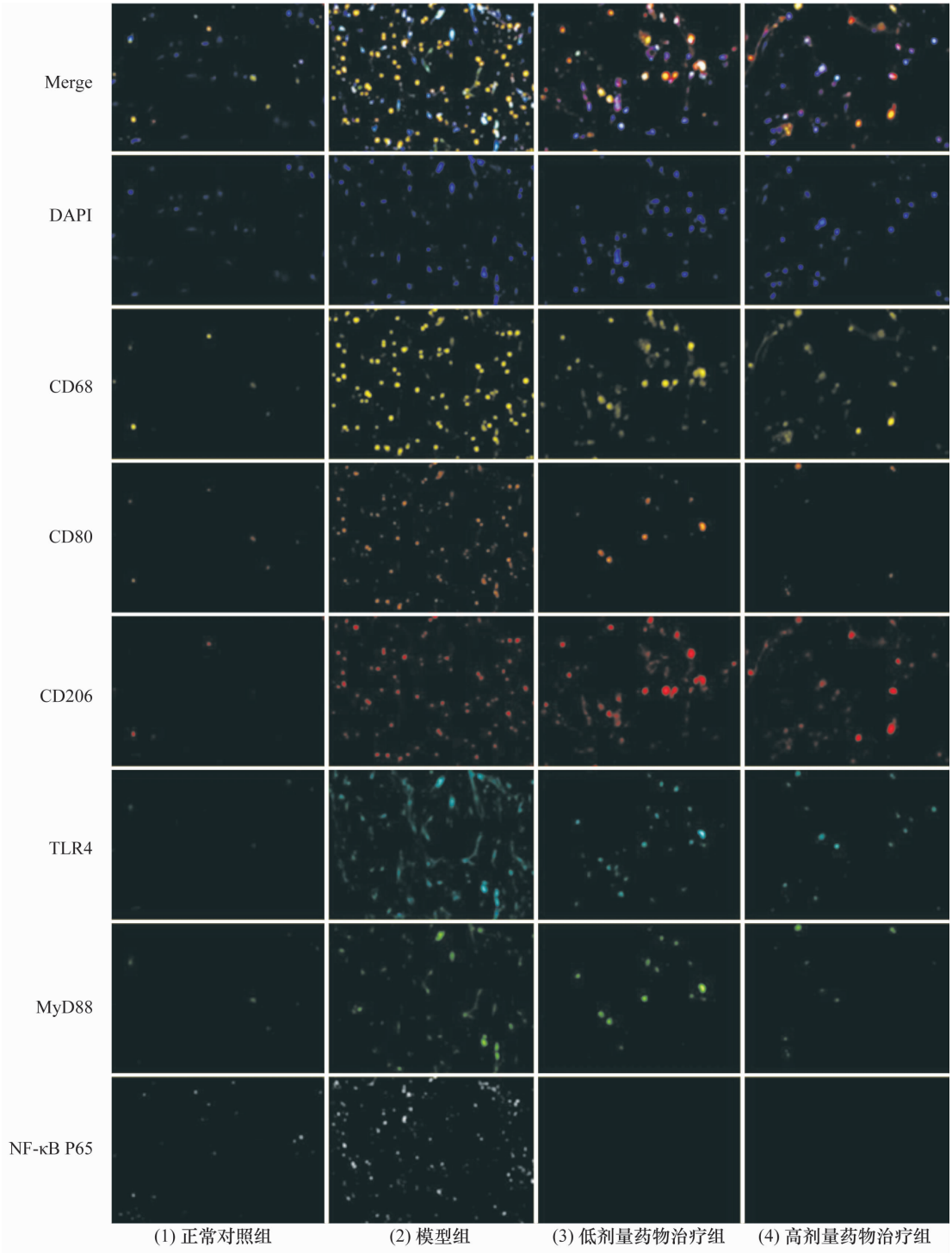

Merge 表示融合图片，DAPI 为 4，6-二脒基-2-苯基吲哚，TLR4 为 Toll 样受体 4，MyD88 为髓样分化因子初次应答基因 88，NF-κB p65 为核因子-κB p65。

图 3　4 组大鼠股骨头巨噬细胞极化及 TLR4/MyD88/NF-κB 信号通路相关蛋白表达多重免疫组化检测结果

4　讨　论

SONFH 属中医学“骨蚀”“骨痿”“骨痹”范畴，其主要证候为肾虚、血瘀。因此，补肾活血是 SONFH 的主要治则。股骨头坏死愈胶囊作为平乐郭氏正骨的经典方剂，临床实践显示其治疗 SONFH 效果显著。该方由鹿茸、丹参、续断、杜仲、黄芪、水蛭、鸡血藤、玄参、连翘、乳香、没药共 11 味药物组成。相关研究表明，杜仲的主要活性成分杜仲苷能够有效抑制SONFH 发病进程[12]，丹参、川芎等活血类中药的有效成分也被证实具有抑制炎症反应的作用[13-14]。但股骨头坏死愈胶囊治疗 SONFH 作用机制尚不清楚。

SONFH 的发生与持续性慢性炎症所导致的骨再

生障碍密切相关,因而 SONFH 的炎症反应机制也成为研究的重点[15]。相关研究发现,M1 型巨噬细胞的过度激活是引起 SONFH 持续性慢性炎症的主要原因[16-17],而 M1 型巨噬细胞不能向 M2 型巨噬细胞极化是导致 SONFH 微环境内持续慢性炎症和组织破坏的关键,在股骨头坏死的进程中起着至关重要的作用[18-20]。骨组织损伤后,骨细胞和骨髓细胞释放的损伤相关模式分子将巨噬细胞招募到损伤区域,并将其极化为 M1 型巨噬细胞,进而促进炎症因子肿瘤坏死因子-α(tumor necrosis factor-α,TNF-α)、白细胞介素(interleukin,IL)-1β、IL-6 的分泌,启动和维持炎症反应,并导致骨修复和再生障碍[21]。而促进 M1 型巨噬细胞向 M2 型巨噬细胞极化,则能够抑制 SONFH 慢性炎症持续、减轻组织破坏,进而促进骨组织的再生与修复[22-23]。TLR4/MyD88/NF-κB 信号通路是调控炎症反应的经典通路,在巨噬细胞的极化过程中发挥重要作用[24-25]。Adapala 等[26]通过研究猪股骨头坏死模型发现,在坏死骨组织引起巨噬细胞向 M1 型巨噬细胞极化过程中,TLR4 的表达量显著增加,且引起了依赖 MyD88 途径的下游信号的改变。Zhu 等[27]研究发现,抑制 TLR4/MyD88/NF-κB 信号通路可以有效抑制炎症因子 TNF-α、IL-1β、IL-6 的释放,抑制炎症反应,促进坏死骨组织内的骨形成,从而延缓 SONFH 进展。我们采用 mIHC 探讨股骨头坏死愈胶囊治疗 SONFH 作用机制,结果显示,模型组大鼠股骨头 M1 型巨噬细胞占比、M2 型巨噬细胞占比均显著上升,TLR4/MyD88/NF-κB 信号通路蛋白表达上调;股骨头坏死愈胶囊治疗后能够显著抑制巨噬细胞向 M1 型极化、促进巨噬细胞向 M2 型极化,能够抑制 TLR4/MyD88/NF-κB 信号通路蛋白表达的上调;且股骨头坏死愈胶囊对巨噬细胞极化及 TLR4/MyD88/NF-κB 信号通路蛋白表达的影响具有一定的浓度依赖性。

本研究结果表明,股骨头坏死愈胶囊治疗 SONFH,能够显著改善股骨头骨微结构、抑制骨坏死,其作用具有一定的剂量依赖性;其作用机制与调控 TLR4/MyD88/NF-κB 信号通路蛋白表达及巨噬细胞极化有关。

参考文献

[1] POWELL C,CHANG C,NAGUWA S M,et al. Steroid induced osteonecrosis:an analysis of steroid dosing risk[J]. Autoimmun Rev,2010,9(11):721-743.

[2] CUI L,ZHUANG Q,LIN J,et al. Multicentric epidemiologic study on six thousand three hundred and ninety five cases of femoral head osteonecrosis in China[J]. Int Orthop,2016,40(2):267-276.

[3] COHEN-ROSENBLUM A,CUI Q. Osteonecrosis of the femoral head[J]. Orthop Clin North Am,2019,50(2):139-149.

[4] 谭旭仪,刘又文,高书图,等. 股骨头坏死愈胶囊治疗股骨颈骨折术后患者 55 例临床观察[J]. 中医杂志,2014,55(4):308-310.

[5] 谭旭仪,刘又文,高书图,等. 股骨头坏死愈胶囊对股骨头坏死患者血液流变学的影响[J]. 中成药,2014,36(10):2227-2228.

[6] KALRA J,BAKER J. Multiplex immunohistochemistry for mapping the tumor microenvironment[J]. Methods Mol Biol,2017,1554:237-251.

[7] SHENG W,ZHANG C,MOHIUDDIN T M,et al. Multiplex immunofluorescence:a powerful tool in cancer immunotherapy[J]. Int J Mol Sci,2023,24(4):3086.

[8] CORTENBACH K R G,MORALES CANO D,MEEK J,et al. Topography of immune cell infiltration in different stages of coronary atherosclerosis revealed by multiplex immunohistochemistry[J]. Int J Cardiol Heart Vasc,2022,44:101111.

[9] PANG L,ERNST M,HUYNH J. Development of a multiplex immunohistochemistry workflow to investigate the immune microenvironment in mouse models of inflammatory bowel disease and colon cancer[J]. Int J Mol Sci,2021,22(20):11001.

[10] TAN Z,WANG Y,CHEN Y,et al. The dynamic feature of macrophage M1/M2 imbalance facilitates the progression of non-traumatic osteonecrosis of the femoral head[J]. Front Bioeng Biotechnol,2022,10:912133.

[11] WU X,YANG S,DUAN D,et al. Experimental osteonecrosis induced by a combination of low-dose lipopolysaccharide and high-dose methylprednisolone in rabbits[J]. Joint Bone Spine,2008,75(5):573-578.

[12] YUE C,JIN H,ZHANG X,et al. Aucubin prevents steroid-induced osteoblast apoptosis by enhancing autophagy via AMPK activation[J]. J Cell Mol Med,2021,25(21):10175-10184.

[13] KOLAC U K,USTUNER M C,TEKIN N,et al. The anti-inflammatory and antioxidant effects of salvia officinalis on lipopolysaccharide-induced inflammation in rats[J]. J Med

Food,2017,20(12):1193 - 1200.

[14] ZHANG H F,WANG Y L,GAO C,et al. Salvianolic acid A attenuates kidney injury and inflammation by inhibiting NF-kappaB and p38 MAPK signaling pathways in 5/6 nephrectomized rats[J]. Acta Pharmacol Sin,2018,39(12):1855 - 1864.

[15] MA M,TAN Z,LI W,et al. Osteoimmunology and osteonecrosis of the femoral head[J]. Bone Joint Res,2022,11(1):26 - 28.

[16] MA M,TAN Z,LI W,et al. Infographic:osteoimmunology mechanism of osteonecrosis of the femoral head[J]. Bone Joint Res,2022,11(1):29 - 31.

[17] WU X,FENG X,HE Y,et al. IL-4 administration exerts preventive effects via suppression of underlying inflammation and TNF-alpha-induced apoptosis in steroid-induced osteonecrosis[J]. Osteoporos Int,2016,27(5):1827 - 1837.

[18] JIN T,ZHANG Y,SUN Y,et al. IL-4 gene polymorphisms and their relation to steroid-induced osteonecrosis of the femoral head in Chinese population[J]. Mol Genet Genomic Med,2019,7(3):e563.

[19] WU X,XU W,FENG X,et al. TNF-a mediated inflammatory macrophage polarization contributes to the pathogenesis of steroid-induced osteonecrosis in mice[J]. Int J Immunopathol Pharmacol,2015,28(3):351 - 361.

[20] ZHENG J,YAO Z,XUE L,et al. The role of immune cells in modulating chronic inflammation and osteonecrosis[J]. Front Immunol,2022,13:1064245.

[21] JIANG C,ZHOU Z,LIN Y,et al. Astragaloside Ⅳ ameliorates steroid-induced osteonecrosis of the femoral head by repolarizing the phenotype of pro-inflammatory macrophages[J]. Int Immunopharmacol,2021,93:107345.

[22] JIN S,MENG C,HE Y,et al. Curcumin prevents osteocyte apoptosis by inhibiting M1-type macrophage polarization in mice model of glucocorticoid-associated osteonecrosis of the femoral head[J]. J Orthop Res,2020,38(9):2020 - 2030.

[23] TIAN G,LIU C,GONG Q,et al. Human umbilical cord mesenchymal stem cells improve the necrosis and osteocyte apoptosis in glucocorticoid-induced osteonecrosis of the femoral head model through reducing the macrophage polarization[J]. Int J Stem Cells,2022,15(2):195 - 202.

[24] WANG Y,WANG K,BAO Y,et al. The serum soluble Klotho alleviates cardiac aging and regulates M2a/M2c macrophage polarization via inhibiting TLR4/Myd88/NF-kappaB pathway[J]. Tissue Cell,2022,76:101812.

[25] CIRMI S,MAUGERI A,RUSSO C,et al. Oleacein attenuates lipopolysaccharide-induced inflammation in THP-1-derived macrophages by the inhibition of TLR4/MyD88/NF-kappaB pathway[J]. Int J Mol Sci,2022,23(3):1206.

[26] ADAPALA N S,YAMAGUCHI R,PHIPPS M,et al. Necrotic bone stimulates proinflammatory responses in macrophages through the activation of Toll-like receptor 4[J]. Am J Pathol,2016,186(11):2987 - 2999.

[27] ZHU D,YU H,LIU P,et al. Calycosin modulates inflammation via suppressing TLR4/NF-kappaB pathway and promotes bone formation to ameliorate glucocorticoid-induced osteonecrosis of the femoral head in rat[J]. Phytother Res,2021,35(5):2824 - 2835.

(收稿日期:2023-10-30 本文编辑:吕宁)

(上接第 22 页)

[12] SHEN S,LIAO Q,LIU J,et al. Myricanol rescues dexamethasone-induced muscle dysfunction via a sirtuin 1-dependent mechanism[J]. J Cachexia Sarcopenia Muscle,2019,10(2):429 - 444.

[13] CHANG J S,KONG I D. Irisin prevents dexamethasone-induced atrophy in C2C12 myotubes[J]. Pflugers Arch,2020,472(4):495 - 502.

[14] LARSON A A,SYVERUD B C,FLORIDA S E,et al. Effects of dexamethasone dose and timing on tissue-engineered skeletal muscle units[J]. Cells Tissues Organs,2018,205(4):197 - 207.

[15] CAIRNS D M,UCHIMURA T,KWON H,et al. Muscle cells enhance resistance to pro-inflammatory cytokine-induced cartilage destruction[J]. Biochem Biophys Res Commun,2010,392(1):22 - 28.

[16] CAIRNS D M,LEE P G,UCHIMURA T,et al. The role of muscle cells in regulating cartilage matrix production[J]. J Orthop Res,2010,28(4):529 - 536.

[17] RAINBOW R S,KWON H,FOOTE A T,et al. Muscle cell-derived factors inhibit inflammatory stimuli-induced damage in hMSC-derived chondrocytes[J]. Osteoarthritis Cartilage,2013,21(7):990 - 998.

[18] PEAKE J M,DELLA GATTA P,SUZUKI K,et al. Cytokine expression and secretion by skeletal muscle cells:regulatory mechanisms and exercise effects[J]. Exerc Immunol Rev,2015,21:8 - 25.

(收稿日期:2023-01-02 本文编辑:李晓乐)